FZJ-IKP(TH)-2000-28

Mapping the proton unintegrated gluon distribution in dijets correlations in real and virtual photoproduction at HERA.

A. Szczurek[1]

[1] *Institute of Nuclear Physics*
PL-31-342 Cracow, Poland

N.N. Nikolaev[2,3], W. Schäfer[2] and J. Speth[2]

[2] *Institut für Kernphysik (Theorie), Forschungszentrum Jülich,*
D-52425 Jülich, Germany
[3] *L.D.Landau Institute for Theoretical Physics*
Chernogolovka, Moscow Region 142 432, Russia

Abstract

We discuss how the dijet azimuthal correlations in DIS and real photoproduction at HERA probe the differential (unintegrated) gluon distribution in the proton. We find a strong dependence of the azimuthal correlation pattern on Bjorken-x, photon virtuality and the cut on the jet transverse momenta. A rise of the azimuthal decorrelations is observed with decreasing Bjorken-x due to the interplay of perturbative and nonperturbative effects. We predict a strong rise of the same-side jet rate with photon energy for real photoproduction. We discuss conditions for the correlation function to be dominated by hard perturbative gluons and ways of constraining the size of the nonperturbative soft component. We make some predictions for the THERA energy range. The analysis of the energy dependence of the isolated jet and two-jet cross sections in photoproduction would be a new way to study the not yet well constrained unintegrated gluon distributions and to explore the onset of the pQCD regime.

1 Introduction

Most of the recent studies of low-x dynamics relevant for HERA concentrated on the analysis of the inclusive structure function, i.e. on the total cross section for $\gamma^* p$ scattering [1] and on diffraction [2]. Because at low x photon-gluon fusion is the dominant underlying mechanism, such studies open the possibility of better understanding the so-called unintegrated gluon distributions, the quantity first introduced in [3].

The jet studies are known to be a good tool to test perturbative QCD effects. It was pointed out already some time ago that dijet production in DIS could be a method to study the onset of BFKL dynamics both in photo- [4] and electroproduction [5]. Unfortunately in practice, due to unavoidable cuts on transverse momenta of jets, one samples rather large values of the gluon longitudinal momentum fraction x_g, where it is not completely clear what is the underlying dynamics and in particular what unintegrated gluon distribution should be used. Up to now mostly real photoproduction data were published by ZEUS and H1 collaborations [7]. Recently the H1 collaboration at HERA made available some new results for jet production [8]. However, in all these analyses only rather inclusive observables have been discussed.

In the present note we discuss the jet production beyond the familiar collinear approximation and focus on how more exclusive and more differential jet production observables probe the unintegrated gluon distribution. Based on the unintegrated gluon distributions found recently [9] from the phenomenological analysis of $\sigma^{tot}_{\gamma^* p}$ we explore dijet azimuthal decorrelations. In Ref.[6] such decorrelation effects were discussed in a perturbative BFKL approach, and as a consequence only decorrelation effects at some distance from the back-to-back configuration could be analyzed. The extension to the whole azimuthal phase space requires understanding the differential gluon densities in non-perturbative soft region. The modelling of the nonperturbative soft gluon exchange as done in Ref.[9] allows us to extend the region of the azimuthal angle between jets closer to π and to explore the onset of the hard regime.

2 The formalism

Here we collect basic formulae used throughout the present note.

At the parton level the total cross section for quark-antiquark dijet production $\gamma^* + p \to j_1 + j_2 + X$ (see Fig.1) can be written in a compact way as:

$$\sigma^{\gamma^* p \to j_1 j_2}_{T/L}(x, Q^2) = \int d\phi \int_{p^2_{1,\perp,min}} dp^2_{1,\perp} \int_{p^2_{2,\perp,min}} dp^2_{2,\perp} \; \frac{f_g(x_g, \kappa^2)}{\kappa^4} \cdot \tilde{\sigma}_{T/L}(x, Q^2, \vec{p}_{1,\perp}, \vec{p}_{2,\perp}) \; , \quad (1)$$

where x and Q^2 are standard kinematical variables. In the formula above $f_g(x_g, \kappa^2)$ is the unintegrated gluon distribution, which will be specified somewhat later, and $\vec{\kappa}$ is the transverse momentum of the exchanged gluon. It is related to the quark/antiquark jet transverse momenta $\vec{p}_{1,\perp}$ and $\vec{p}_{2,\perp}$ as:

$$\vec{p}_{2,\perp} = \vec{\kappa} - \vec{p}_{1,\perp} \; , \; \kappa^2 = p^2_{1,\perp} + p^2_{2,\perp} + 2 p_{1,\perp} p_{2,\perp} cos\phi \; . \quad (2)$$

We have written explicitly lower cuts on the transverse momenta of jets in (1). The indices T and L refer to transverse and longitudinal photons, respectively. The auxilliary quantities

introduced in (1)

$$\tilde{\sigma}_T(x,Q^2,\vec{p}_{1,\perp},\vec{p}_{2,\perp}) = \frac{\alpha_{em}}{2}\cdot\int dz \sum_f e_f^2\alpha_s(l^2)$$
$$\left\{[z^2+(1-z)^2]\left|\frac{\vec{p}_{1,\perp}}{p_{1,\perp}^2+\varepsilon_f^2}+\frac{\vec{p}_{2,\perp}}{p_{2,\perp}^2+\varepsilon_f^2}\right|^2+m_f^2\left(\frac{1}{p_{1,\perp}^2+\varepsilon_f^2}-\frac{1}{p_{2,\perp}^2+\varepsilon_f^2}\right)^2\right\} \quad (3)$$

for transverse photons and

$$\tilde{\sigma}_L(x,Q^2,\vec{p}_{1,\perp},\vec{p}_{2,\perp}) = \frac{\alpha_{em}}{2}\cdot\int dz\sum_f e_f^2\alpha_s(l^2)\left\{4Q^2z^2(1-z)^2\left(\frac{1}{p_{1,\perp}^2+\varepsilon_f^2}-\frac{1}{p_{2,\perp}^2+\varepsilon_f^2}\right)^2\right\} \quad (4)$$

for longitudinal photons. Above we introduced

$$\varepsilon_f^2 = z(1-z)Q^2+m_f^2\,. \quad (5)$$

The unintegrated gluon distribution f_g is evaluated at

$$x_g = \frac{M_t^2+Q^2}{W^2+Q^2}\,, \quad (6)$$

where

$$M_t^2 = \frac{p_{1,\perp}^2+m_f^2}{z}+\frac{p_{2,\perp}^2+m_f^2}{1-z} \quad (7)$$

is flavour dependent. It is obvious then that at large transverse momenta of jets one samples larger values of x_g than in the case of total cross section. The scale of the running coupling constant in (3) and (4) is taken to be $l^2=\max(\kappa^2,\varepsilon_f^2+p_j^2)$, where for small l^2 the coupling constant is frozen as in [9].

The gluon momentum κ is responsible for the jets being not exactly back-to-back in contrast to the conventional collinear approximation to leading order. In the following we limit ourselves to the region of $x_\gamma\sim 1$, where the jets are dominantly produced from the quark box on the very top of the gluonic ladder. In doing so we restrict ourselves to leading order parton calculation and omit jets from the ladder.

The principal issue is how the isolated single jet and dijet production samples the unintegrated gluon distribution and when the azimuthal correlation function will be dominated by hard perturbative gluons. Although in the present note we address this question based on the unintegrated gluon distribution $f_g(x_g,\kappa^2)$ from a recent analysis in [9] where it was modelled phenomenologically to describe structure function data at low Bjorken-x and the total cross section for real $\gamma+p$ scattering, we believe that our principal conclusions are to a great extent model-independent. The following simple two-component Ansatz was adopted in [9]

$$f_g(x_g,\kappa^2) = \mathcal{F}_{soft}(\kappa^2)\frac{\kappa_s^2}{\kappa^2+\kappa_s^2}+\mathcal{F}_{hard}(x_g,\kappa^2)\frac{\kappa^2}{\kappa^2+\kappa_h^2}\,. \quad (8)$$

The parameters κ_s and κ_h determine the scale of the transition from the hard to soft gluon region [9].

The soft nonperturbative component was chosen in the Born form

$$\mathcal{F}_{soft}(\kappa^2) = a_{soft} C_F N_c \frac{\alpha_s}{\pi} V(\kappa^2) \frac{\kappa^4}{(\kappa^2 + \mu^2_{soft})^2} \ . \tag{9}$$

The vertex function $V(\kappa^2)$ is expressed by the single-body isoscalar nucleon form factor

$$V(\kappa^2) \approx 1 - F(3\kappa^2) \ . \tag{10}$$

The standard dipole parametrization for F was used.

The hard component was taken in the form

$$\mathcal{F}_{hard}(x_g, \kappa^2) = \mathcal{F}^{(B)}(\kappa^2) \frac{\mathcal{F}_{pt}(x_g, Q_c^2)}{\mathcal{F}^{(B)}(Q_c^2)} \theta(Q_c^2 - \kappa^2) + \mathcal{F}_{pt}(x_g, \kappa^2) \theta(\kappa^2 - Q_c^2) \ , \tag{11}$$

where $\mathcal{F}^{(B)}$ is of the Born form (see [9]). The not yet specified $\mathcal{F}_{pt}$ is calculated from known conventional DGLAP parametrizations as

$$\mathcal{F}_{pt}(x_g, \kappa^2) = \frac{\partial G_{DGLAP}(x_g, \kappa^2)}{\partial \log \kappa^2} \ . \tag{12}$$

The results presented in this note were obtained based on a recent MRST98 LO parametrization [12]. As an example in Fig.2 we show the resulting unintegrated gluon distribution as a function of κ^2 for a few different values of x_g. The x_g-independent soft component is shown separately by the dashed line. The model in [9] is limited to small $x_g \ll 0.1$ only, and should not be applied for $x_g > 0.03$. For other technical details we refer the reader to [9].

The two-component structure (8) of the unintegrated gluon distribution as displayed in Fig.2 leads to interesting consequences for the dijet azimuthal correlations which will be studied in the following section. The hard/soft decomposition of the gluon distribution found in [9] is sufficiently generic to believe that our major conclusions on the onset of the hard regime are not strongly model dependent and are relevant also to BFKL driven models.

3 Results

3.1 Dijets

In the present note we shall discuss mainly the effect of azimuthal jet-jet correlations and leave the effect of other correlations for a separate analysis. We shall limit ourselves to study the region of small Bjorken-x only. The cross section for the dijet production strongly depends on cuts imposed on kinematical variables. In order to better demonstrate the effect of coexistence of perturbative and nonperturbative effects in the following analysis we shall restrict ourselves to cuts on kinematical variables in the so-called hadronic center of mass (HCM) sytem (γ^*-proton center of mass). In the present purposefully simplified analysis we impose the cuts on the parton level and avoid extra cuts in the laboratory frame.

In Fig.3, we present $d\sigma(\gamma^* p \to j_1 j_2)/d\phi$ as a function of HCM azimuthal angle between jets for two different values of photon virtuality $Q^2 = 4$ GeV^2 (left panel) and $Q^2 = 16$ GeV^2 (right panel) for a series of Bjorken x. In this calculation, we have restricted the transverse momenta of jets to $p^{HCM}_{1,\perp}, p^{HCM}_{2,\perp} > p_{t,cut} = 4$ GeV and summed over light flavours u, d and s.

While in the case of the total cross section the effective mass m_f of the quark is responsible for confinement effects, in the dijet production the cross section is in practice independent of the explicit value of m_f. One can observe a strong dependence of the azimuthal angle decorrelation pattern on Bjorken x. A closer inspection of both panels simultaneously leads to the conclusion that averaging over a broad range of Q^2 would to a large extent destroy the effect as it involves automatically averaging over a certain range of x_g, the most crucial variable for the effect to be observed. A significant part of the effect is due to the interplay of the hard(perturbative) and soft(nonperturbative) components. This is explained better in Fig.4 where the correlation function is decomposed into hard and soft components for two rather different values of Bjorken-x: $x = 10^{-4}$ (left panel) and $x = 5 \cdot 10^{-3}$ (right panel). In this calculation the virtuality of the photon was fixed to $Q^2 = 8$ GeV^2. While at $x = 10^{-4}$ the hard component dominates, at larger x the soft component becomes equally important. In the region of small ϕ and small x our results are similar to those from perturbative BFKL dynamics [5], which is rather a general feature of the $k_\perp$-factorization approach.

The onset of the hard regime can be best seen in the lower part of Fig.4 where we present averaged value of the gluon transverse momentum κ (solid line) as sampled at different azimuthal angle ϕ between jets. For comparison we also show average transverse momentum of the harder ($p_{\perp,hard} = \max(p_{1,\perp}, p_{2,\perp})$, long-dashed line) and softer ($p_{\perp,soft} = \min(p_{1,\perp}, p_{2,\perp})$, short-dashed line) quark(antiquark) jet. The region of small azimuthal angle ϕ (same-side jets) samples on average rather large values of gluon transverse momentum κ where the perturbative component dominates. Here on average gluon transverse momentum is larger than the transverse momentum of each of the two jets. At $\phi = 0$, $< \kappa > = < p_{\perp,hard} > + < p_{\perp,soft} >$. In our case ($x_\gamma \sim 1$) the momentum of the same-side jets $\vec{\kappa}$ is compensated by the transverse momentum of hadrons (minijets) which carry a very small fraction of photon's momentum. Close to $\phi = \pi$ the average κ is rather small, smaller than the transverse momentum of each of the jets. In this region, models for the soft component can be tested.

In the case of symmetric cut in a sharp (in κ^2) transition between soft and hard region, to a crude approximation, the hard region can be estimated as $\cos\phi > -1 + \kappa_0^2/2p_{t,cut}^2$, where κ_0 is the transition value in the gluon transverse momentum. In the model in [9], the border is not as well defined and the transition region depends in addition on x_g. We wish to mention that in general the region of larger ϕ ($|\phi - \pi| \sim 0$) is model dependent. In our model, the cross section depends on the treatment of the infra-red region i.e. the formula used for α_s and the choice of its argument. We hope that studying this region experimentally could provide new information about genuine nonperturbative effects which are rather poorly known up to now.

The cut on the transverse momentum is usually a tool to define jets. Studying the dependence of the result on the cut may however provide some new information. As an example in Fig.5 we show the dependence of $d\sigma/d\phi$ on the cut on the HCM transverse momenta of jets for fixed value of $x = 10^{-3}$ and $Q^2 = 8$ GeV^2 and in Fig.6 the corresponding decomposition into soft and hard components for $p_{t,cut} = 2$ GeV (left panel) and $p_{t,cut} = 6$ GeV (right panel). The small $p_{t,cut} = 2$ GeV may be slightly academic but is chosen here to better emphasize the effect. In both cases we observe the dominance of the hard component at small ϕ and the soft component near to the back-to-back configuration. In the traditional collinear approximation such a separation of soft and hard component is not possible as they are both lumped together into the integrated gluon density. In the collinear approximation in first order in α_s, jets are produced back-to-back and only higher order corrections lead to an azimuthal decorrelation. By comparing the two panels in Fig.4 one can observe stronger back-to-back correlations for

larger $p_{t,cut}$. This is due to the fact that the larger p_t region is unavoidably related to larger x_g, that is to the region of f_g in which the soft component is more prominent.

The experimental identification of the effects discussed here requires good statistics in the data sample. Up to now, in practice [10], one averages rather over broader range of Bjorken x, photon virtuality and jet transverse momenta. Most of the effects discussed in the present note are then washed out and the information about the small-x dynamics is to a large extent lost. It seems rather difficult at present to study the whole correlation function $w(\phi)$ for fixed values of x and Q^2. We suggest that at present, instead of analyzing $w(\phi)$ itself, one could study the ratio:

$$S(x,Q^2) \equiv \frac{\int_0^{\pi/2} w(\phi; x, Q^2, p_{t,cut})\; d\phi}{\int_0^{\pi} w(\phi; x, Q^2, p_{t,cut})\; d\phi}\;, \tag{13}$$

i.e. the percentage of the same-side dijets of all dijets, as a function of Bjorken-x, photon virtuality Q^2 and/or the cuts on transverse momenta of jets $p_{t,cut}$. In Table 1, we show as an example the predictions of the two-component model [9] for S as a function of Bjorken-x and $p_{t,cut} = 4$ GeV. Here the virtuality of the photon was fixed at $Q^2 = 8$ GeV^2. As seen from the table, the two-component model predicts a significant dependence of the same-side jet fraction S on Bjorken-x and the value of the lower cut-off on jet transverse momenta in HCM. The larger Bjorken x, the lower S and the smaller $p_{t,cut}$, the larger S. In fact these two effects are at least partially correlated. It should be noticed that the larger $p_{t,cut}$ means automatically the larger x_g (see Eq.(6)). These strong effects predicted here should be easy to observe experimentally. However, a more detailed comparison with experimental data should include the separation of jets in rapidity/azimuthal angle space [1] and/or hadronization effects. The higher-order QCD corrections are expected to increase S, especially for larger values of x and/or larger cuts on transverse momenta, i.e. in the region where it is small.

In the model in Ref.[9] the total (real) photoproduction cross section at energies $W <$ 100 GeV is dominated by the soft component. Only at very high, not yet available, energies the hard component would dominate. At "intermediate" energy available at HERA, the two components coexist and their fraction is a smooth function of initial γp energy. In principle, the same stays true for the dijet production and has interesting consequences for the jet azimuthal correlations. In Fig.7, we show the azimuthal correlation for a few different values of γp center of mass energy $W = 50$, 100, 200, 500 GeV. We observe strongly rising decorrelation of jets when going from fixed target energies to energies relevant at THERA [13]. Similarly as in the jet electroproduction, the key variable here is the gluon momentum fraction, which is $< x_g > \approx 5{\cdot}10^{-2}$ at W = 50 GeV and $< x_g > \approx 10^{-3}$ at the THERA energy of 500 GeV. We get $S \approx$ 0.5% at W = 50 GeV. At the THERA energy of 500 GeV we predict about 3.5% of the same side jets. The rise of the decorrelation with the photon energy in real photoproduction can be traced back to larger values of κ sampled by the same-side jets than by the opposite-side jets. We note that the rise of the decorrelation with increasing energy obtained here based on the model from [9], is rather typical of $k_\perp$-factorization approach in general. Therefore the experimental confirmation of this effect would be a valuable test of this kind of approach.

[1] This is more important for the same-side jets.

3.2 Isolated jets in the photon hemisphere

There is another interesting prediction of the two-component model which we wish to discuss briefly now. Up to now we have discussed only cases when both jets have transverse momenta larger than a certain cut value $p_{t,cut}$. In principle there are also cases (events) with one hard ($p_\perp > p_{t,cut}$) jet and one soft ($p_\perp < p_{t,cut}$) "jet". In this single jet event $x_\gamma < 1$, because the transverse momentum of the single quark(antiquark) jet is compensated by a transverse momentum of a much softer gluon. [2] In the following we shall call such cases "one jet" events for simplicity, as opposed to the previous case called here "two jet" events for brevity. Let us compare the rate of such "one jet" events to the previously discussed cases of two hard jets in photoproduction. As an example in Fig.8 we compare the cross section for the two cases with the lower cut on transverse momentum $p_{t,cut} = 4$ GeV. Firstly, we observe that the cross section for both cases are of similar order. Furthermore we observe a significantly stronger rise of the cross section for the "one jet" case than for the "two jet" case which may be a bit surprising at least at first look. This different energy dependence is related to different x_g and κ sampled in both cases. For example for W = 100 GeV and $p_{t,cut} = 4$ GeV in the "one jet" case $< x_g > \approx 0.01$ is substantially lower than in the "two jet" case $< x_g > \approx 0.02$. Both numbers are, however, substantially larger than average $< x_g > \approx 0.005$ sampled in the case of total cross section. The effect of κ is more complicated as averaged κ strongly depends on ϕ for the "two jet" case. The interplay of the two effects (x_g and κ) causes the unintegrated gluon distributions to be sampled differently in the "one jet" and "two jet" cases. This, at least potentially, allows the possibility of a further nontrivial test of unintegrated gluon distributions. It would be valuable to compare the present predictions with the predictions of standard (collinear) NLO approach (see for instance [14]).

4 Conclusions

Based on the recent model determination [9] of the unintegrated gluon distribution in the proton we have explored the impact of the soft gluon component and the onset of the perturbative regime on the dijet azimuthal correlations. We have predicted a strong dependence of the azimuthal correlation pattern on Bjorken x, photon virtuality and the cut on the jet transverse momenta. The effects in the electroproduction could be verified now at HERA, provided a careful differential (x ,Q^2, transverse momentum cut) studies of the dijets are made.

In real photoproduction we have predicted the rise of the same-side jet rate with the photon energy. It would be important to compare the results of the model discussed here with the result of the standard collinear approach to understand the potential of such a dijet study to shed more light on the low-x dynamics which has been studied up to now in rather inclusive processes. Finally, we have found that the study of the energy dependence of the "one jet" (defined in the text) cross section would be a new test of unintegrated gluon distributions.

Acknowledgments One of us (A.S.) is indebted to Maciej Przybycień for a discussion of the ZEUS experimental results, Anna Staśto for an exchange of information about some details of their calculation [6] and Igor Ivanov for assistance in using his routine for f_g [9]. This work was partially supported by the German-Polish DLR exchange program, grant number

[2] The dijets quark-gluon and antiquark-gluon can be separated out by cuts on x_γ and/or cuts on rapidities.

POL-028-98.

References

[1] N.N. Nikolaev, B.G. Zakharov and V.R. Zoller, JETP Lett. **66** (1997) 138;
J. Kwieciński, A.D. Martin and A.M. Staśto, Phys. Rev. **D56** (1997) 3991;
H.G. Dosch, T. Gousset and H.J. Pirner, Phys. Rev. **D57** (1998) 1666;
N.N. Nikolaev and V.R. Zoller, JETP Lett. **69** (1999) 103;
E. Gotsman, E. Levin, U. Maor and E. Naftali, Eur. Phys. J. **C10** (1999) 689;
J.R. Forshaw, G. Kerley and G. Shaw, Phys. Rev. **D60** (1999) 074012;
A.D. Martin, M.G. Ryskin and A.M. Staśto, Eur. Phys. J. **C7** (1999) 643;
K. Golec-Biernat and M. Wüsthoff, Phys. Rev. **D59** (1999) 014017.

[2] M. Bertini, M. Genovese, N.N. Nikolaev, A.V. Pronyaev and B.G. Zakharov, Phys. Lett. **B422** (1998) 238;
K. Golec-Biernat and M. Wüsthoff, Phys. Rev. **D60** (1999) 114023;
J.R. Forshaw, G.R. Kerley and G. Shaw, Nucl. Phys. **A675** (2000) 80.

[3] V.S. Fadin, E.A. Kuraev and L.N. Lipatov, Phys. Lett. **B60** (1975) 50;
E.A. Kuraev, L.N. Lipatov and V.S. Fadin, Sov. Phys. JETP **44** (1976) 443; **45** (1977) 199.

[4] J.R. Forshaw and R.G. Roberts, Phys. Lett. **B335** (1994) 494.

[5] A.J. Askew, D. Graudenz, J. Kwieciński and A.D. Martin, Phys. Lett. **B338** (1994) 92.

[6] J. Kwieciński, A.D. Martin and A.M. Staśto, Phys. Lett. **B459** (1999) 644.

[7] S. Aid et al.(H1 coll.), Z. Phys. **C70** (1996) 17;
M. Derrick et al.(ZEUS coll.), Phys. Lett. **B384** (1996) 401;
J. Breitweg et al.(ZEUS coll.), Eur. Phys. J. **C1** (1998) 109;
J. Breitweg et al.(ZEUS coll.), Eur. Phys. J. **C11** (1999) 35;
C. Adloff et al.(H1 coll.), Phys. Lett. **B483** (2000) 36.

[8] C. Adloff et al. (H1 Collaboration), hep-ex/0010054.

[9] I.P. Ivanov and N.N. Nikolaev, hep-ph/0004206.

[10] M. Przybycień, Phd thesis, Kraków, 1998.

[11] S.P. Baranov and N.P. Zotov, Phys. Lett. **B491** (2000) 111.

[12] A.D. Martin, R.G. Roberts, W.J. Stirling and R.S. Thorne, Phys. Lett. **B443** (1998) 301.

[13] M. Klein, Talk given at 8th International Workshop on Deep Inelastic Scattering and QCD, DIS2000; Liverpool, April 2000; to appear in the proceedings.

[14] E. Mirkes and D. Zeppenfeld, Phys. Lett. **B380** (1996) 105;
B.W. Harris and J.F. Owens, Phys. Rev. **D56** (1997) 4007;
S. Frixione and G. Ridolfi, Nucl. Phys. **B507** (1997) 315;
G. Kramer and B. Pötter, Eur. Phys. J. **C5** (1998) 665.

	$p_{t,cut}(GeV)$		
Bjorken-x	2	4	6
$1 \cdot 10^{-4}$	6.41(-0)	2.30(-0)	9.35(-1)
$2 \cdot 10^{-4}$	5.07(-0)	1.58(-0)	5.66(-1)
$5 \cdot 10^{-4}$	3.42(-0)	8.13(-1)	2.23(-1)
$1 \cdot 10^{-3}$	2.34(-0)	4.00(-1)	6.68(-2)
$2 \cdot 10^{-3}$	1.46(-0)	1.34(-1)	2.54(-3)
$5 \cdot 10^{-3}$	6.72(-1)	5.83(-3)	———
$1 \cdot 10^{-2}$	3.15(-1)	———	———

Table 1: The fraction of the HCM same-side jets $S(x, Q^2, p_{t,cut})$ in % as the function of Bjorken-x and the symmetric cut on the jet transverse momenta in GeV for $Q^2 = 8$ GeV^2.

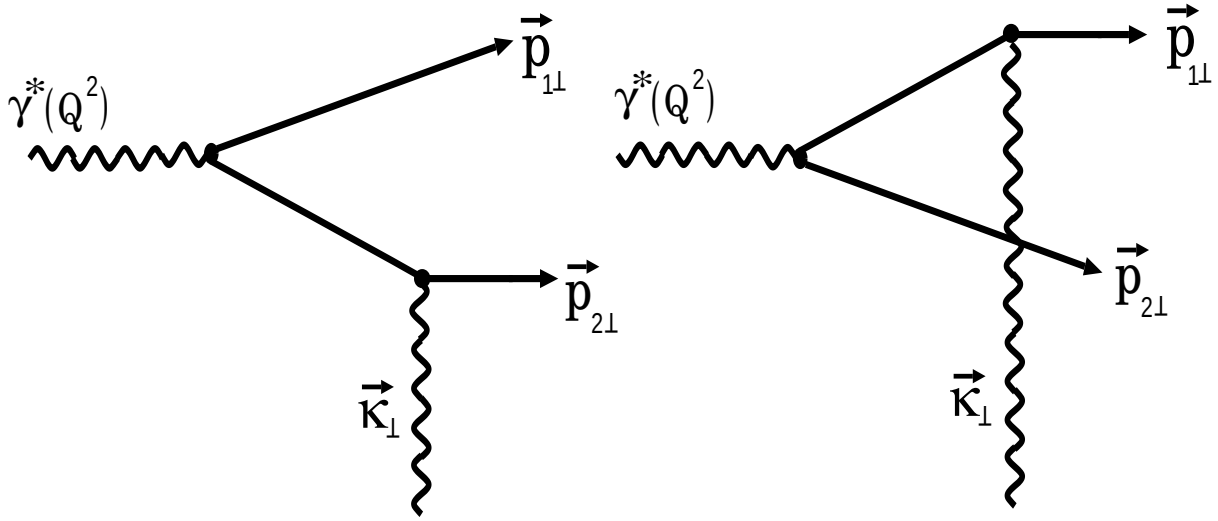

Figure 1: Dijet production via photon-gluon fusion. $\vec{\kappa_\perp}$ is the gluon transverse momentum.

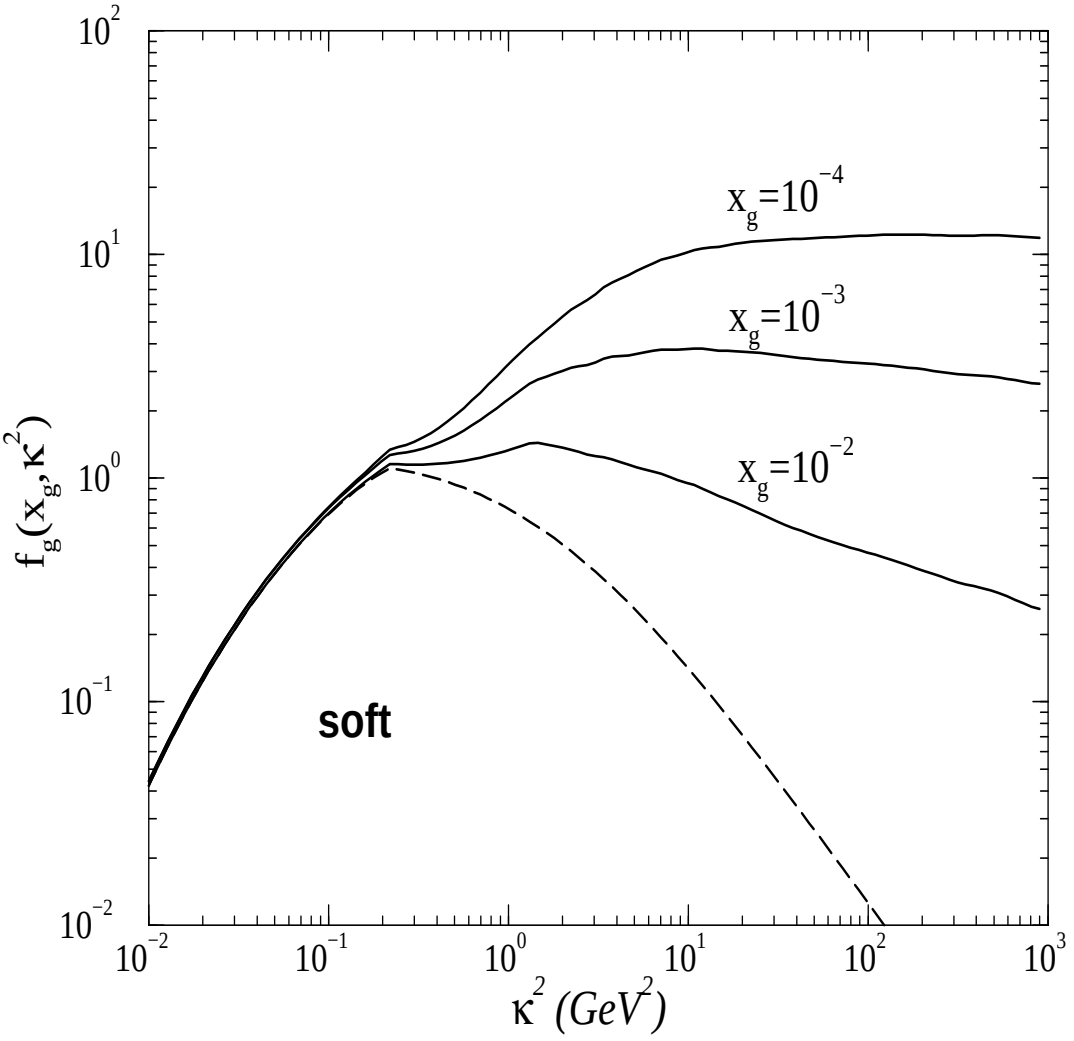

Figure 2: The unintegrated gluon distribution as a function κ^2, for different values of x_g.

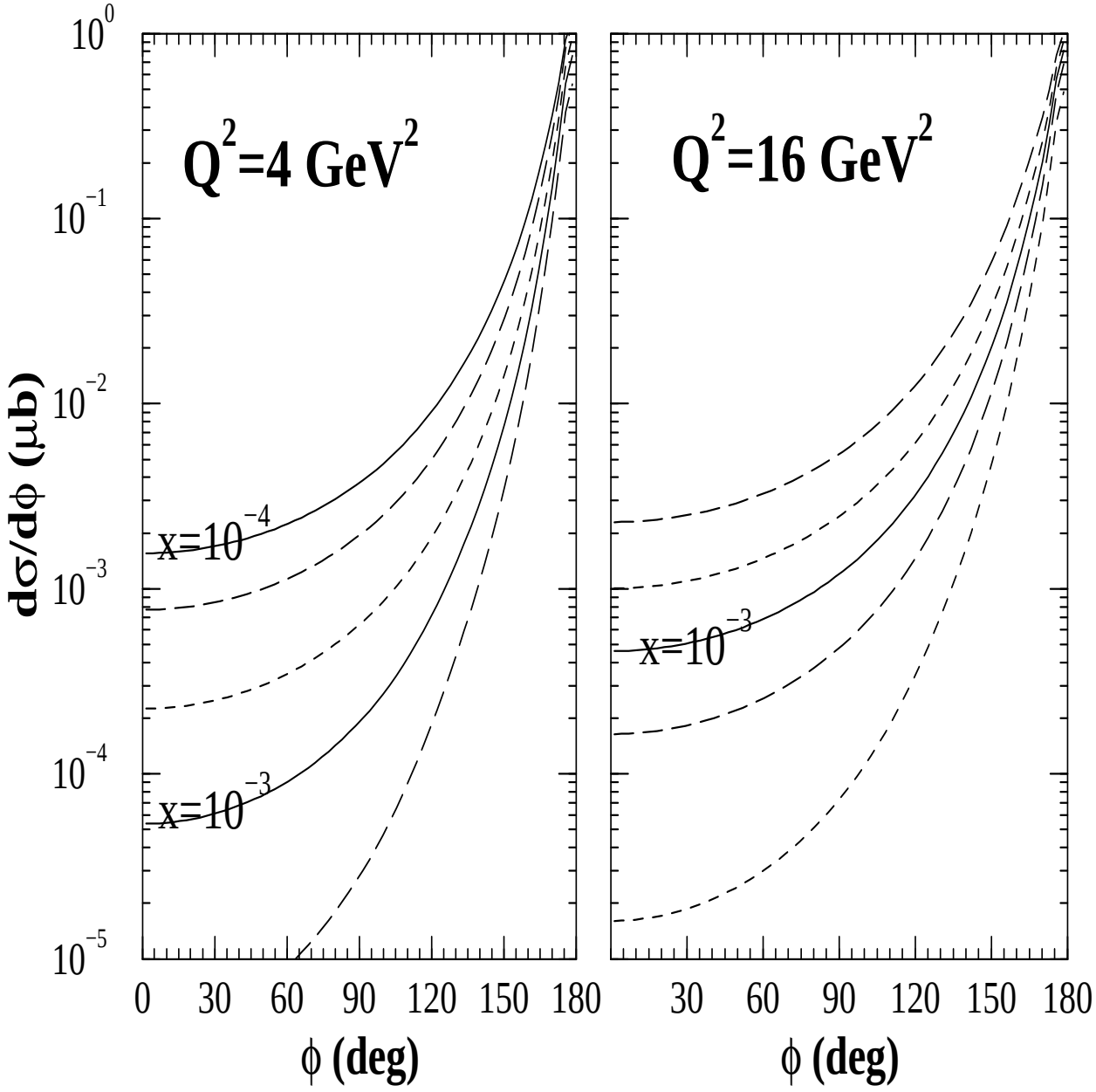

Figure 3: The cross section for $\gamma^* p \to j_1 j_2$ as a function of HCM azimuthal angle between jets for $Q^2 = 4$ GeV^2 (left panel) and $Q^2 = 16$ GeV^2 (right panel) for several values of Bjorken-x $= 10^{-4}$ (solid), $2 \cdot 10^{-4}$ (long-dashed), $5 \cdot 10^{-4}$ (short-dashed), 10^{-3} (solid), $2 \cdot 10^{-3}$ (long-dashed), $5 \cdot 10^{-3}$ (short-dashed).

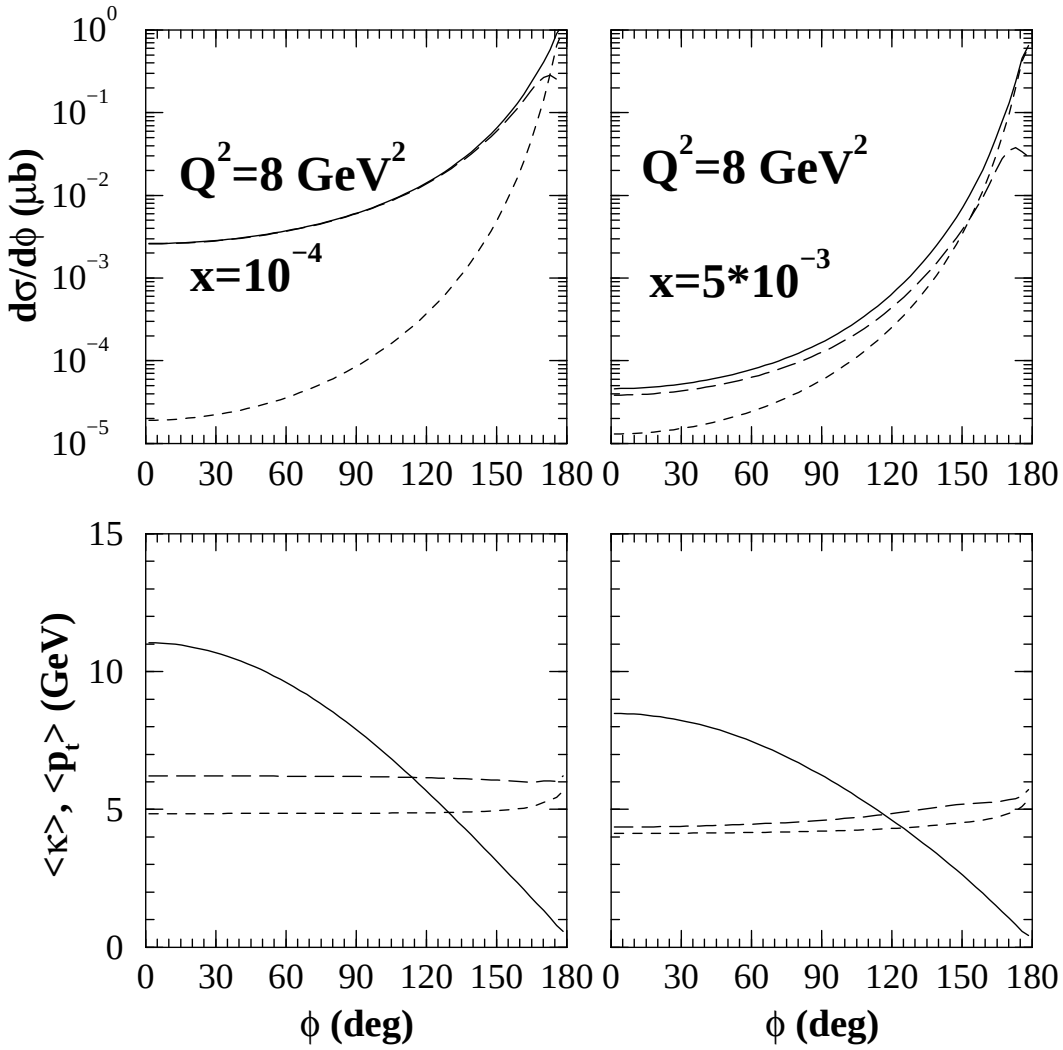

Figure 4: The decomposition of the HCM azimuthal correlation function $w(\phi)$ into hard (long-dashed) and soft (short-dashed) components for $x = 10^{-4}$ (upper left panel) and $x = 5{\cdot}10^{-3}$ (upper right panel). In this calculation $Q^2 = 8$ GeV^2 and $p_{t,cut} = 4$ GeV. In the lower panels, the average gluon transverse momentum $< \kappa >$ (solid line) and $p_{\perp,soft}$ (short-dashed line) and $p_{\perp,hard}$ (long-dashed line) are shown correspondingly.

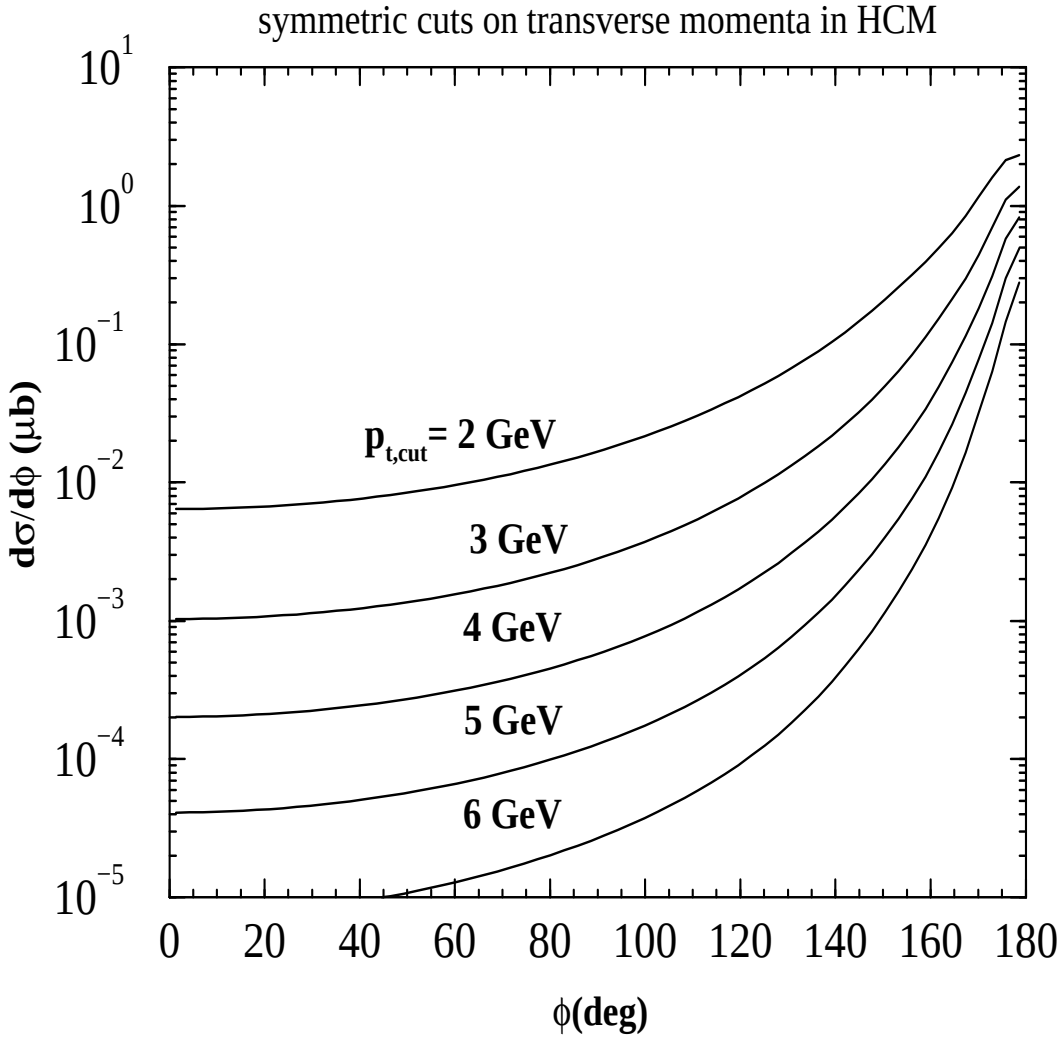

Figure 5: The cross section for $\gamma^* p \to q\bar{q}$ as a function of HCM azimuthal angle between jets for $Q^2 = 8$ GeV^2, $x = 10^{-3}$ for several values of the HCM symmetric cut on the jet transverse momenta: $p_{t,cut}$ = 2,3,4,5,6 GeV.

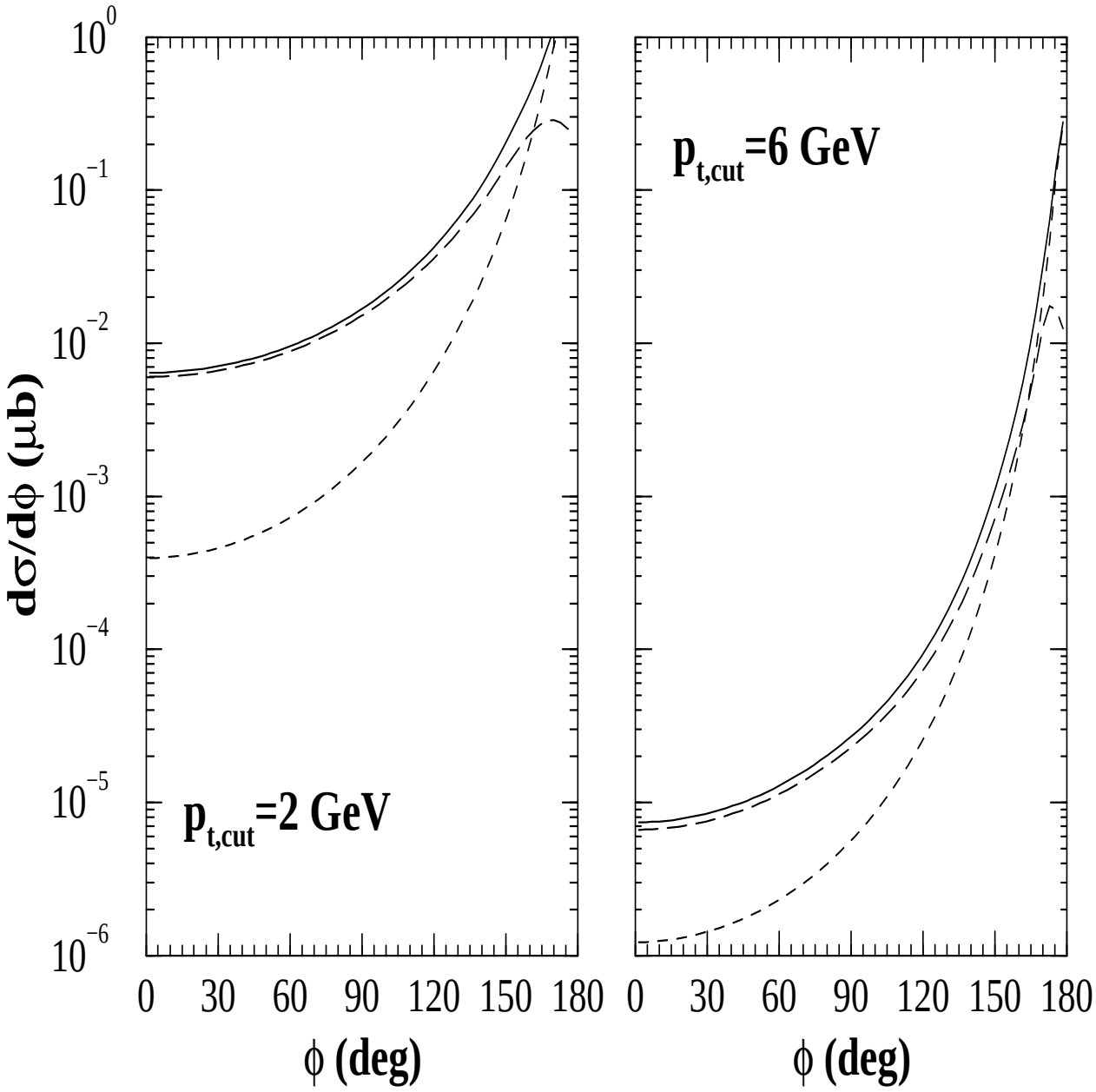

Figure 6: The decomposition of the HCM azimuthal correlation function $w(\phi)$ into hard (long-dashed) and soft (short-dashed) components for $p_{t,cut} = 2$ GeV (left panel) and $p_{t,cut} = 6$ GeV (right panel). In this calculation $Q^2 = 8$ GeV^2 and $x = 10^{-3}$.

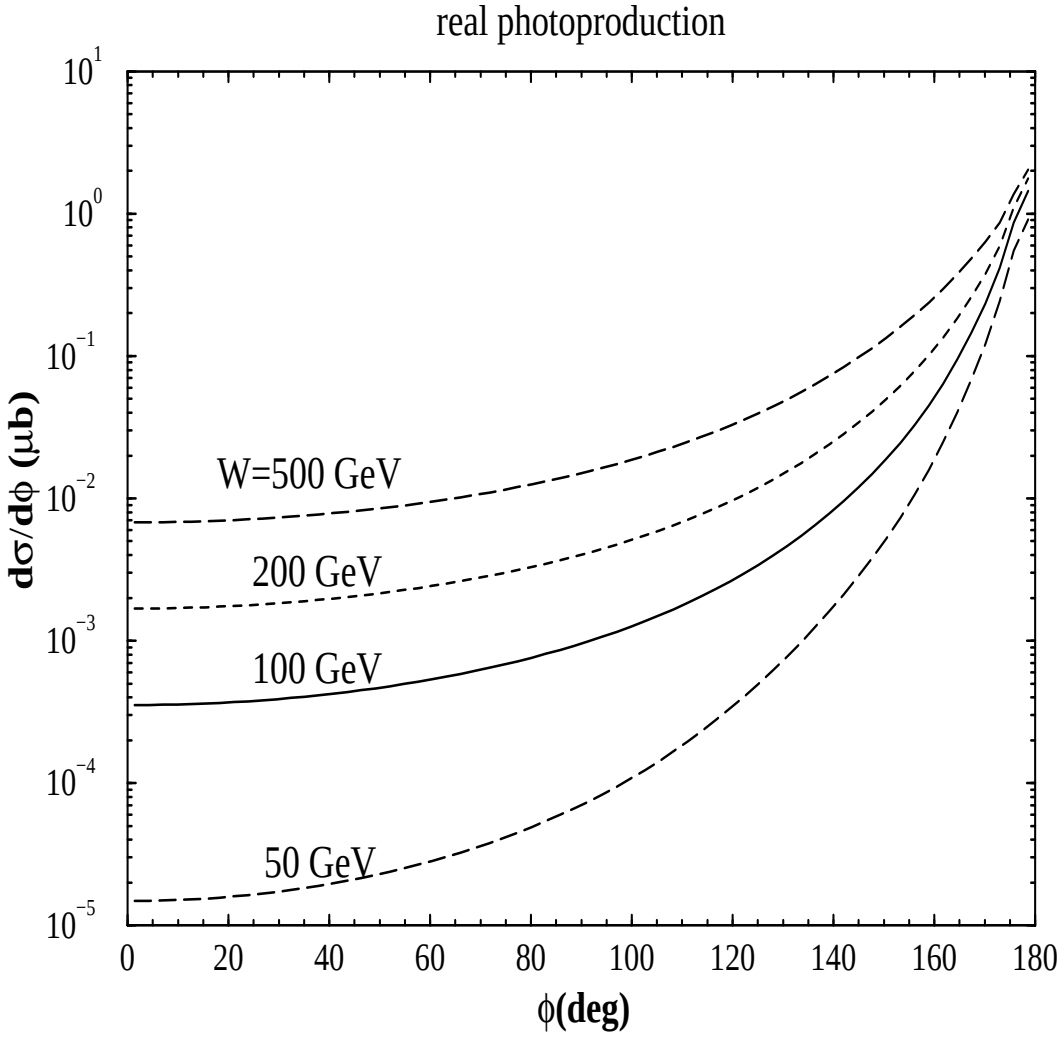

Figure 7: The correlation function of dijets in real photoproduction for different γp center-of-mass energies W = 50, 100, 200, 500 GeV. In this calculation a lower cut on both jets momenta $p_{t,cut}$ = 4 GeV was imposed.

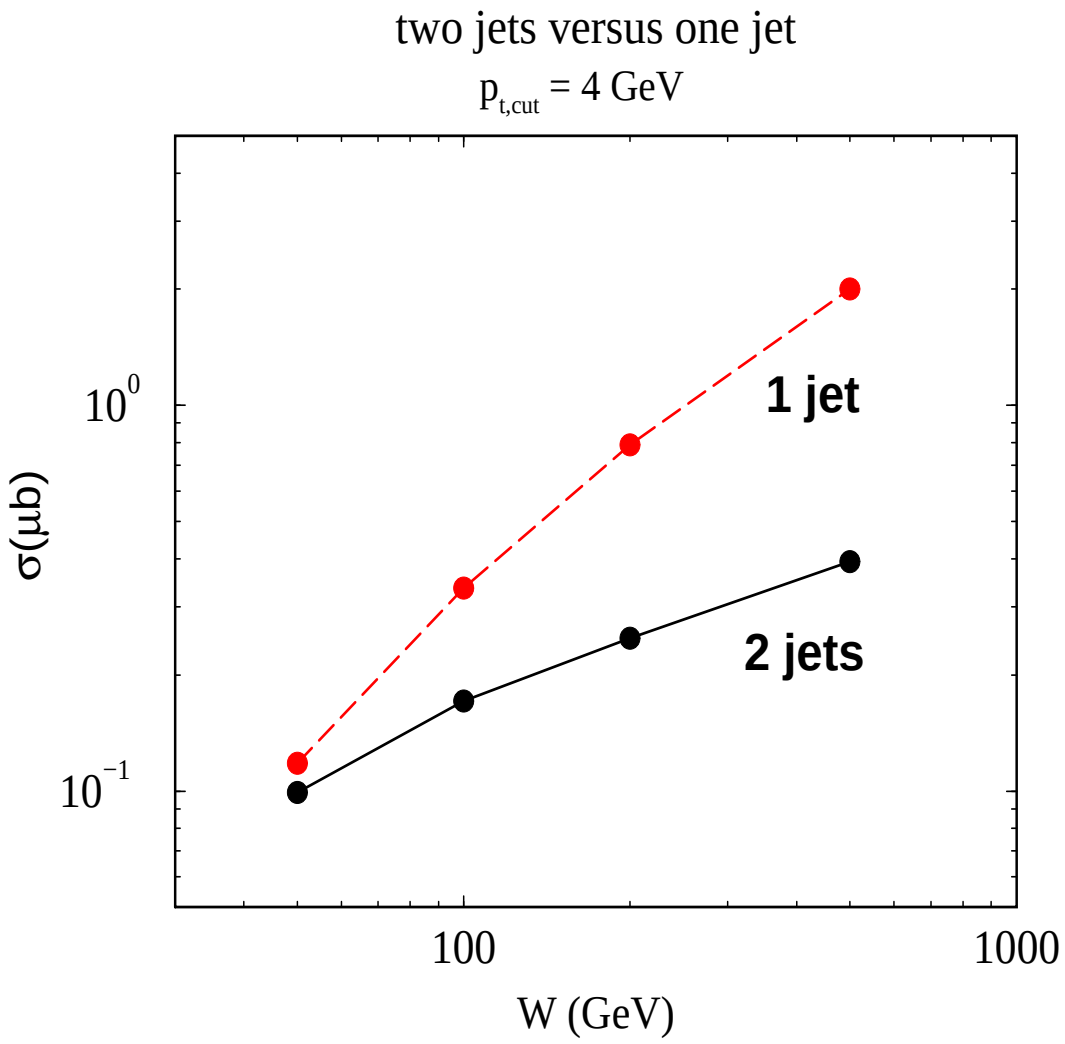

Figure 8: The cross section for $\gamma p \rightarrow$ "two jet" (solid) and "one jet" (dashed) cases as a function of γp CM energy. In this calculation $p_{t,cut} = 4$ GeV.